The infrared spectrum of Neptune at 3.5-4.1 microns: Search for H3+ and evidence for recent meteorological variations

Helmut Feuchtgruber, Thérèse Encrenaz

A&A 403, L7–L10 (2003)
DOI: 10.1051/0004-6361:20030414

Astronomy & Astrophysics

The infrared spectrum of Neptune at 3.5–4.1 microns: Search for H_3^+ and evidence for recent meteorological variations⋆

H. Feuchtgruber[1] and Th. Encrenaz[2]

[1] Max-Planck-Institut für extraterrestrische Physik, Postfach 1603, 85740 Garching, Germany
[2] LESIA, Observatoire de Paris, 5 place Janssen, 92195 Meudon Cedex, France
e-mail: Therese.Encrenaz@obspm.fr

Received 24 February 2003 / Accepted 19 March 2003

Abstract. The infrared spectrum of Neptune at 3.5−3.75 μm and 3.87−4.1 μm has been measured at a spectral resolution of 1200. The observed flux is stronger by a factor ∼3 compared to previous measurements, suggesting important meteorological variations between 1997 and 2002. The flux is detected mostly from a bright belt at mid-southern latitudes. Strong absorptions, identified as methane, are observed over the *L* band. The observed CH_4 spectrum can be fitted by a multilayer model assuming that the solar light is partly reflected above several layers, including the CH_4 haze and stratospheric photochemical hazes. An upper limit to a disk averaged column density of H_3^+ of $2.9\left(^{+7.1}_{-1.8}\right) \times 10^{10}$ cm^{-2} is reported, consistent with present ionospheric models.

Key words. line: formation – radiative transfer – planets and satellites: individual: Neptune – infrared: solar system

1. Introduction

As compared to Uranus, Neptune exhibits surprisingly strong atmospheric activity, characterized, in particular, by the contrast and variability of its visual spots, and by the large amount of stratospheric methane which implies supersaturation. The presence of a significant internal source of energy on Neptune (Pearl & Conrath 1991) appears to be sufficient to counterbalance its low solar energy input and to generate strong dynamical activity.

The near infrared flux of Neptune can show substantial variability (Joyce et al. 1977; Lockwood & Thompson 2002) on time scales from days to years with largest observed amplitudes in the *K* and *L* bands. In addition to long-term variations which seem to show a correlation with solar activity, two unusually strong disturbances have been detected in the near-infrared range, the first one in 1976 and the second one in 1986–1989 (Baines et al. 1995b; Lockwood & Thompson 2002). These variations are thought to originate from significant albedo changes probably caused by the formation of stratospheric aerosols produced by methane photochemistry. The 1977 disturbance might have been caused by an increase of aerosol production, possibly connected to an external meteoritic source (Moses 1992). The 1986–1989 phenomenon, in contrast, might have been associated with a tropospheric event caused by rapid convective upwelling (Hammel et al. 1992).

In this letter, we report new observations of portions of the 3–4 μm spectrum of Neptune which show evidence for a strong flux increase on a time scale of a few years. These data were first acquired in an attempt to detect H_3^+ in Neptune's ionosphere as this ion, already found in the three other giant planets (Drossart et al. 1989; Geballe et al. 1993; Trafton et al. 1993), is still undetected on Neptune. Section 2 describes the observations. Section 3 shows the spectrum of Neptune at 3.5–4.1 μm and describes its interpretation in the frame of a multilayer model of Neptune's atmosphere. Section 4 gives an upper limit to the H_3^+ abundance on Neptune and compares it with theoretical ionospheric models. Our conclusions are summarized in Sect. 5.

2. Observations and data reduction

Observations were carried out with the ISAAC imaging spectrometer at the UT1 (ANTU) of the Very Large Telescope at the European Southern Observatory in Cerro Paranal (Chile). The spectra were acquired in the LWS3-MR medium resolution mode with the 2″ slit resulting in a spectral resolution of about $\lambda/\Delta\lambda = 1200$. Motivated by a search for H_3^+, two individual grating settings were chosen to cover the wavelength ranges from 3.5 μm to 3.75 μm and from 3.87 μm to 4.11 μm. The spectra were measured on 17 August 2002 03:48:06–06:58:30 UT and 19 August 2002 03:17:57–06:50:08 UT at a subsolar latitude of −28.5°, including acquisition images and calibration observations of standard stars. The total exposure

Send offprint requests to: H. Feuchtgruber, e-mail: fgb@mpe.mpg.de
⋆ Based on observations obtained at the European Southern Observatory, Paranal, Chile, within the observing program 70.C-0004(A).

times on Neptune were 148 and 175 min, respectively. The range of airmasses went from 1.0 to 1.4 during both observations and the measured average *V*-band seeing was 0.7″ during the first and 1.0″ during the second night. Two standard stars, HD 214080 and HD 205905, were observed for telluric corrections and absolute flux calibration of the Neptune spectra.

Since every observation was split into 3 separate observation blocks, the data reduction was carried out individually for each block. The processing has been done following Amico et al. (2002). Dark subtraction, non-linearity correction, flatfielding, A–B subtraction for chopped and nodded images and the slit curvature correction have been implemented by our own IDL routines. However the master flat data and the 2D polynomial coefficients describing the slit curvature were taken from the ISAAC pipeline processing results. All individual spectroimages were registered and shifted on top of each other to remove the offsets introduced by the chopping jitter. The wavelength calibration was derived starting from the ISAAC pipeline wavelength scale and the spectra of the Xe and Ar arc lamps, by fitting Gaussians to the individual spectral lines for center determinations. The offsets between the fitted and tabulated values of the arc lines allowed a significant 3rd order polynomial correction to the pipeline calibration. After removing $\geq 3\sigma$ outliers from the stacked spectroimages, the signal to noise of the observation has been further improved by inverting and coadding the negative spectroimages to the positive data before the extraction of the spectrum. The extracted three spectra of the individual observation blocks were then averaged.

The same processing has been applied to the data for the calibration standards HD 214080 and HD 205905. In this wavelength range, these standards have been considered as ideal blackbodies with $T_{\rm eff}$ = 24 300 K and L' = 7.257 mag for HD 214080 (Conlon et al. 1993) and $T_{\rm eff}$ = 5616 K and 1.97 Jy at 4.2 μm for HD 205905 (Johnson & Wright 1983). Finally the Neptune spectra have been divided by the standards. We believe that the uncertainty in the absolute flux calibration of the two spectra derived by this procedure is about 10%. Although both spectra have been obtained within 8° at the same subearth longitudes, typical rotational periods of features on Neptune are about 18.3 hours (Lockwood & Thompson 2002) resulting in approximately 135° difference. Therefore their fluxes may not necessarily match to each other, since the known (e.g. Joyce et al. 1977) photometric *L*-band variability within one rotation period could account for a factor of ∼1.5. The long wavelength part of the Neptune spectrum has been scaled by a factor 0.75 for matching the absolute flux scale to the first part of the spectrum and for allowing a consistent modelling of both parts.

From *K*-band acquisition images (4 s exposures) taken prior to and in between the observation blocks, two mid-latitude belt like regions are identified, with the southern one being much stronger. For an example see Fig. 1a. Most of the spectral signal originates from that southern region, confirmed by the relative intensity profile along the slit (Fig. 1b) during the actual *L*-band spectra acquisition. We note that such a spatial distribution has been previously observed in the past, with the equatorial belt being weaker than those at higher latitudes, and the southern belt being typically brighter than its northern counterpart (Baines et al. 1995b). The *K*-band seeing derived from the same images by fitting the *FWHM* of Triton is ∼0.38″.

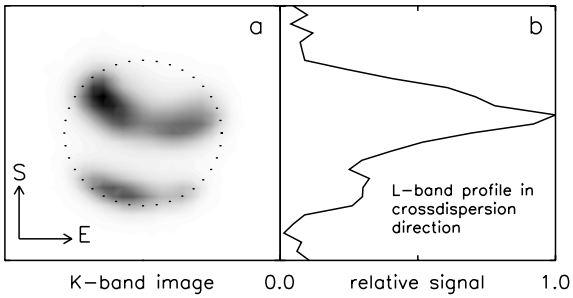

Fig. 1. a) ISAAC *K*-band target acquisition image of Neptune. The dotted circle has a diameter of 2.35″. **b)** Relative signal profile in cross-dispersion direction during spectral *L*-band observation.

3. The CH_4 spectrum between 3.5 μm and 4.1 μm

Figure 2 shows the observed spectrum of Neptune in the *L* band. The first comment to be made is that the observed flux is about 3 times higher than observed in May 1997 by the PHT-S instrument of the Infrared Space Observatory (ISO). These low-resolution observations (R = 90) provided a detection of Neptune's flux at 2.7 μm at a level of 0.02 Jy, and an upper limit of about 0.01 Jy in the 3.2–4.2 μm range (Encrenaz et al. 2000). The ISAAC data, of much better signal-to-noise ratio, indicate a flux level of 0.03 Jy at 3.7 μm. The increase of Neptune's angular diameter between the two observations implies a flux increase of 10%, and longitudinal variations in the *L* band should not exceed about 50% (Joyce et al. 1977); we thus interpret the excess flux as the signature of recent meteorological variations. In addition, the increased signal-to-noise ratio and spectral resolving power of our data (R = 1200) allow a clear detection of several absorption features which can all be attributed to methane.

In order to interpret these data, we have calculated synthetic spectra of Neptune using a radiative transfer model. The atmospheric model of Neptune, already used for fitting the ISO data at 2.5–4.2 μm (Encrenaz et al. 2000), was taken from Baines et al. (1995a, 1995b). This model assumes (1) a lower cloud layer at about 3 bars, presumably made of H_2S ice, (2) a CH_4 cloud ranging between 0.3 and 1.5 bars, and (3) a haze of hydrocarbons (mostly C_2H_6 and C_2H_2) around 0.01 bars. The tropospheric mixing ratio of CH_4 is 0.022, corresponding to an enhancement by a factor of about 30 with respect to the solar value, as expected from the nucleation model of the planet (Gautier et al. 1995). Above the CH_4 cloud, methane exhibits supersaturation. We assumed a stratospheric mixing ratio of 5×10^{-4}, as a mean estimate derived from the previous determinations in the UV range with Voyager (Bishop et al. 1998) and the infrared range with ISO (Bézard et al. 1999).

As in the case of the reduction of the ISO spectrum (Encrenaz et al. 2000), we used a line-by-line, reflecting-layer calculation, including the CH_4 data bases of GEISA (Jacquinet-Husson et al. 1997), Hilico et al. (1994) and Wenger & Champion (1998), with a total number of more

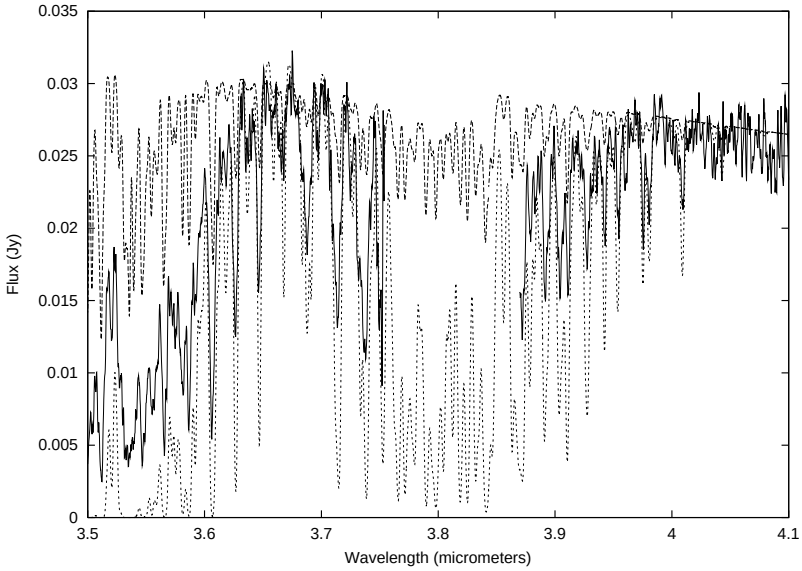

Fig. 2. Observed *L*-band spectrum of Neptune (solid) and synthetic spectra corresponding to two models: (1) reflection over a lower cloud (P = 0.1 bar), presumably associated to the CH_4 saturation level (dotted); reflection over an intermediate cloud (P = 0.01 bar), presumably associated with hydrocabon condensation (dashed).

than 70 000 lines. A Voigt profile was used in our calculations in the vicinity of the line centers. For the far wings of CH_4, we used the shape factor derived by Hartmann (priv. comm.) from a laboratory analysis of CH_4 around 3 μm, which introduces a depletion of the absorption coefficient at frequency distances larger than 26 cm^{-1} from the line center (Encrenaz et al. 2000).

As a first step, we calculated the synthetic spectrum of Neptune above a single cloud, located at different altitudes. Figure 2 shows a comparison of our data with two extreme cases: (1) P = 0.1 bar ([CH_4] = 750 cm-am); (2) P = 0.01 bar ([CH_4] = 75 cm-am). It can be seen that the radiation of Neptune comes from intermediate levels between these two clouds. Figure 3 shows that an intermediate case (P = 0.03 bar, [CH_4] = 250 cm-am) does not provide a good fit to the data, especially in the short-wavelength range and in addition, there is no simple physical interpretation for this intermediate cloud (Baines et al. 1995a).

A much better fit is obtained if a multilayer model is used. Figure 3 shows a synthetic spectrum based on a model which incorporates 3 components: (1) reflection over the lower cloud level at 0.1 bar with an albedo contribution of 70%; (2) reflection over the intermediate cloud at 0.01 bar with an albedo contribution of 24%; (3) reflection over a high-stratospheric haze (above the 1 mbar level) with an albedo contribution of 6%. Although this combination is obviously not unique, it provides a good description of the observed spectrum with a plausible model of Neptune's atmosphere. The lower cloud would correspond to the upper level of the CH_4 cloud (although slightly higher than in Baines et al.'s model). The intermediate cloud would correspond to the stratospheric aerosol layer due to hydrocarbons (C_2H_6, C_2H_2, possibly C_3H_6 and C_3H_8), in agreement with Baines et al.'s model, while the upper stratospheric haze would correspond to the top of the layer corresponding to HCN and possibly C_4H_2.

Using the absolute flux measurement of our spectrum, and the spatial information provided by Fig. 1, it is possible to derive estimates for the albedos of the 3 different layers. In the case of the 1997 ISO data, we inferred that the best fit corresponded to a model including a high-altitude haze, distributed over the entire planet, with an albedo of 0.002 and a set of CH_4 cirrus covering 0.4% of the planet with an albedo of 0.5. However we were not able to determine these two last parameters independently, because we had no information on the spatial distribution of the infrared flux. In the case of the ISAAC data, taking into account the factor 3 increase in the global flux with respect to the ISO data, its spatial distribution as observed in Fig. 1, and the atmospheric model inferred above, we can derive the following estimates. The global albedos of the 3 levels are found to be respectively 0.008 for the lower cloud, 0.003 for the intermediate cloud, and 0.0007 for the upper haze. Assuming, from Fig. 1, that the southern belt covers about 10% of the total disk, and that the northern belt covers about 5% of it, we infer estimates of 0.05, 0.02 and 0.005 respectively for the albedos of the lower cloud, the intermediate cloud and the upper haze, assuming that the 3 layers show the same local distribution as suggested by Fig. 1. Again, we should re-emphasize that these numbers are no more than plausible estimates, as our proposed atmospheric model is not unique.

4. Upper limit to H_3^+ abundance

To date, the H_3^+ ion has been detected on all giant planets but Neptune. Despite previous observational efforts within the ν_2 rovibrational band (Trafton et al. 1993), no spectral detection could be obtained. Here we report new, more sensitive observations, around the strongest lines of H_3^+ in the wavelength ranges from 3.5 μm to 3.75 μm and from 3.87 μm to 4.11 μm. The minimum detectable lines in our spectra are around 2–2.5$\times 10^{-22}$ W cm^{-2}, which corresponds to the faintest detected CH_4 lines within the same range. In order to translate this limiting flux into an upper limit for a global column density we estimate the ionospheric temperature at the peak of the H_3^+ density profile in the Lyons (1995) model by linear extrapolation from the value at 10^{-8} bar (Bishop et al. 1992) to 10^{-10} bar. The resulting temperature of 550 ± 100 K is consistent with Broadfoot et al. 1989. According to the list of H_3^+

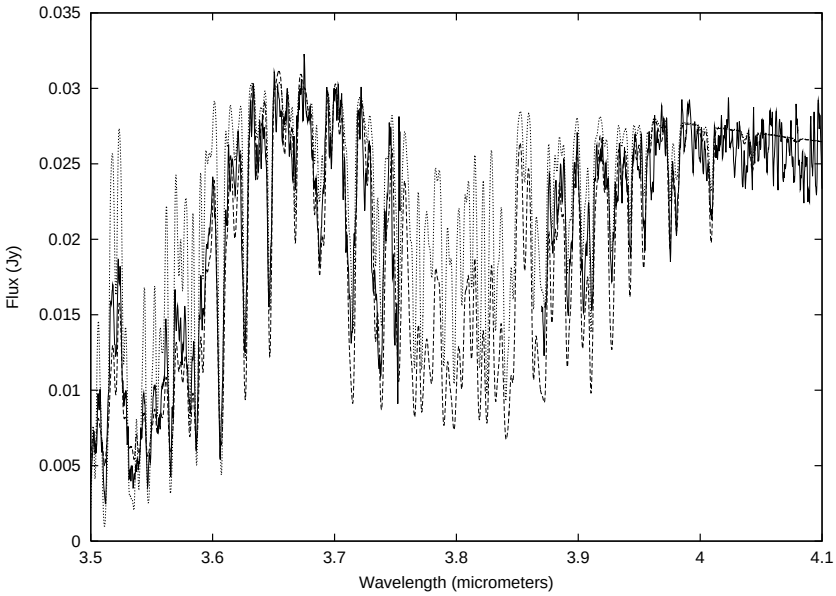

Fig. 3. Observed *L*-band spectrum of Neptune (solid) and synthetic spectrum for the multilayer model (dashed) and the single cloud model calculated for an intermediate case ($P = 0.03$ bar) (dotted).

transitions by Kao et al. 1991 the unresolved doublet lines at 3.953 μm and 3.986 μm are expected to be strongest for this temperature range. Calculating upper limits for the above temperature range gives $2.9\left(^{+7.1}_{-1.8}\right) \times 10^{10}$ cm^{-2} assuming isothermal, optically thin emission. From the ionospheric model of Lyons (1995), a column density of $4\text{–}5 \times 10^9$ cm^{-2} can be expected, therefore our non-detection is consistent with theoretical predictions.

5. Conclusions

In August 2002, we have obtained a near-infrared spectrum of Neptune which shows a significant flux increase with respect to previous data recorded at the same wavelength in 1997. From fitting the CH_4 absorption bands in this spectral range, we can derive that the observed flux comes from different cloud layers, all located at the altitude or above the condensation CH_4 level. The stratospheric layers are likely to be associated with hydrocarbon and HCN hazes produced by photochemistry. The excess of infrared flux is likely to be associated with an increased production of photochemical aerosols, especially along the southern mid-latitude belt as illustrated in Fig. 1. The presence of this strong southern belt is probably connected to the present geometry of Neptune whose southern pole is presently close to the sub-solar point. This result would thus confirm that Neptune's meteorology is actually linked to the variation of the solar incident flux, as was previously suggested by the observed correlation between the visible photometry of Neptune and the solar activity cycle.

Our non-detection of H_3^+ in Neptune appears to be consistent with the predictions inferred from ionospheric models. However H_3^+ removal processes by H_2O caused by meteoritic ablation are significantly overestimated in that model (Lyons 1995), since the adopted influx rates have been taken from Moses (1992), while Feuchtgruber et al. (1997) reported about a factor 10 less input flux of oxygen. Our upper limit could thus be used as an additional constraint for future theoretical work.

References

Amico, P., Cuby, J. G., Devillard, N., Jung, Y., & Lidman, C. 2002, ISAAC Data Reduction Guide 1.5

Baines, K. H., Mickelson, M. E., Larson, L. E., & Ferguson, D. W. 1995, Icarus, 114, 328

Baines, K. H., Hammel, H. B., Rages, K. A., Romani, P. N., & Samuelson, R. E. 1995, in Neptune and Triton, ed. D. P. Cruikshank (University of Arizona Press), 489

Bézard, B., Feuchtgruber, H., & Encrenaz, Th. 1999, ESA SP-427, 153

Bishop, J., Romani, P. R., & Atreya, S. K. 1998, Planet. Space Sci., 46, 1

Bishop, J., Atreya, S. K., Romani, P. N., et al. 1992, J. Geophys. Res., 97, E7, 11681

Broadfoot, A. L., Atreya, S. K., Bertaux, J. L., et al. 1989, Science, 246, 1459

Conlon, E. S., Dufton, P. L., Keenan, F., et al. 1993, A&A, 272, 243

Drossart, P., Maillard, J.-P., Caldwell, J., et al. 1989, Nature, 340, 539

Encrenaz, Th., Schulz, B., Drossart, et al. 2000, A&A, 358, L83

Feuchtgruber, H., Lellouch, E., de Graauw, T., et al. 1997, Nature, 389, 159

Gautier, D., Conrath, B. J., Owen, T., de Pater, I., & Atreya, S. K. 1995, in Neptune and Triton, ed. D. P. Cruikshank (University of Arizona Press), 547

Geballe, T. R., Jagod, M. F., & Oka, T. 1993, ApJ, 408, L109

Hammel, H. B., Lawson, S. L., Harrington, J., et al. 1992, Icarus, 99, 363

Hilico, J.-C., Champion, J.-P., Toumi, S., et al. 1994, J. Mol. Spectr., 168, 455

Jacquinet-Husson, N., Arié, E., Ballard, J., et al. 1997, JQSRT, 62, 205

Johnson, H. M., & Wright, C. D. 1983, ApJS, 53, 643

Joyce, R. R., Pilcher, C. B., Cruikshank, D. P., & Morrison, D. 1977, ApJ, 214, 657

Kao, L., Oka, T., Miller, S., & Tennyson, J. 1991, ApJS, 77, 317

Lockwood, G. W., & Thompson, D. T. 2002, Icarus, 156, 37

Lyons, J. R. 1995, Science, 267, 648

Moses, J. I. 1992, Icarus, 99, 368

Pearl, J. C., & Conrath, B. J. 1991, Geophys. Res. Lett., 96, 18921

Trafton, L. M., Geballe, T. R., Miller, S., et al. 1993, ApJ, 405, 761

Wenger, Ch., & Champion, J.-P. 1998, JQSRT, 59, 471